Chapter 4
Structural Dynamics Identification using Physics-Informed SINDy

Celso T. do Cabo, Raymond Joshua, and Zhu Mao

Abstract Inverse problems in engineering, such as performing system identification and obtaining the Partial Differential Equations (PDEs) of a system is challenging. While it is possible to correlate experimental measurements with a Finite Element Model (FEM) and use the adjusted FEM as a digital twin, it is difficult to obtain such parameters only from measurements. For instance, it is possible to obtain the natural frequencies, mode shapes and damping ratio of a vibrational system using traditional signal processing techniques, but the governing equations may not be easily obtained. With the increase application of machine learning techniques, a specific algorithm developed for system identification is the Sparse Identification of Nonlinear Dynamics (SINDy), which uses the measured signal and its derivatives to estimate the parameters of its PDEs in a matrix form. This work applies SINDy to identify the PDEs of a vibrational system, which consists of second order PDEs. Considering the nature of the problem, the technique is also updated to include physical knowledge of the structure, such as its total mass and first natural frequency, leading to the final estimation of the mass matrix to not be a normalized estimation, allowing the correct estimation of mass, stiffness and damping matrices, as well as a good reconstruction of the original measurement and correct estimation of mode shapes and natural frequencies from the obtained parameters.

Keywords Machine Learning · System Identification · Sparse Identification · Nonlinear Dynamics · Structural Dynamics

Introduction

Inverse problems in engineering, including system identification and obtaining the partial differential equations (PDEs) of a structure can be challenging. Many studies were performed aiming to identify system behavior for linear and nonlinear systems. Some of the approaches for dynamical systems can include regression models, neural networks and fuzzy logic [1, 2]. More recently, with the increase of neural network applications, the Physics Informed Neural Networks (PINNs), were also employed in system identification [3, 4]. However, among the linear regression types, Sparse Identification of Nonlinear Dynamics (SINDy) proposed by Brunton et al. shows great potential for system identification [5]. This technique requires measurements and its derivatives or integrals to obtain the governing equations of a system. Some of the applications for the technique include systems with one degree of freedom (DOF) [6, 7], or in rotary machinery for load identification [8]. Nonlinear normal modes (NNM) of discrete systems were also investigated using SINDy [9]. In addition, other studies were performed on systems with implicit dynamics [10] or in different methodologies to perform the optimization for SINDy, such as employing Runge-Kutta [11] or Gaussian process (GP) for force estimation [12].

However, vibrational systems pose higher complexity, since they possess second order PDEs behavior. Although SINDy has been employed for PDEs applications previously [13]. When dealing with structural dynamics, where continuous systems

NSC-614-5662 10/2024
Unclassified Unlimited Release

Celso T. do Cabo · Zhu Mao (✉)
Department of Mechanical and Materials Engineering Worcester Polytechnic Institute, Worcester, MA 01609
e-mail: ctdocabo@wpi.edu; zmao2@wpi.edu

Raymond Joshua
Honeywell Federal Manufacturing & Technologies, LLC operates the Kansas City, National Security Campus for the United States Department of Energy/National Nuclear, Security Administration under Contract Number DE-NA0002839
e-mail: rjoshua@kcnsc.doe.gov

Brandon Dilworth et al. (eds.), *Topics in Modal Analysis & Parameter Identification II, Vol. 10*, Conference Proceedings of the Society for Experimental Mechanics Series, https://doi.org/10.13052/97887-438-0155-9_4

will lead to dependent mass and stiffness, the estimation of the governing equations poses to be challenging. This work proposes a modification of the traditional SINDy, aiming to perform a system identification of a continuous vibrational system, based on sparse measurements. For that, the modification of the algorithm is given by modifying the linear regression to a stochastic gradient descent (SGD) and including penalty terms to the loss function such that the parameters obtained are encouraged to behave similarly to what would be observed from a finite element (FE) model after reducing its observations to the number of sensors obtained.

Theory Background

To obtain the partial differential equations (PDEs) of a system, the sparse identification of nonlinear dynamics (SINDy) originally proposes a linear regression from the measurements obtained and a library of possible combinations of parameters to obtain the governing equation. For the case of a second order system, the acceleration measurements $\left[\ddot{X}\right]$ is the result that the equation tries to obtain; by integrating the measurements it is possible to build the library of parameters $\Theta\left(\dot{X}, X\right)$ which will consist of the velocity and displacement measurements. By performing the linear regression as shown in Eq. (1), it is possible to estimate the parameters Ξ.

$$\Xi = \left(\Theta^T \Theta\right)^{-1} \Theta^T \ddot{X} \tag{1}$$

The parameters Ξ will then possess the stiffness and damping coefficients normalized by the mass of the system. However, this approach assumes that the mass is independent between the degrees of freedom (DOFs) of the structure and the mass matrix will be composed by an identity matrix. For a more realistic representation of the system, it is proposed a modification in the original algorithm so that the mass matrix is similar to what is expected for vibrational systems, the overall process to obtain the governing equations is presented on the flowchart in Fig. 1. To include the mass matrix in the library of parameters, it is required to modify the original SINDy model from a linear regression to an optimization form. For that, it was chosen to perform a stochastic gradient descent (SGD), and the new library of possible parameters will be changed to $\Theta\left(\ddot{X}, \dot{X}, X\right)$, so that it also has the mass parameters of the system. To optimize the model using SGD, the gradient of the mean squared error must be computed, and it is calculated based on Eq. (2).

$$\nabla_\xi f_{MSE}\left(\ddot{x}, \hat{\ddot{x}}, \xi\right) = \frac{1}{n}\Theta\left(\Theta^T \Xi + b - \ddot{X}\right) \tag{2}$$

where b is the bias of the model. Finally, the values of the parameters will be updated based on Eq. (3).

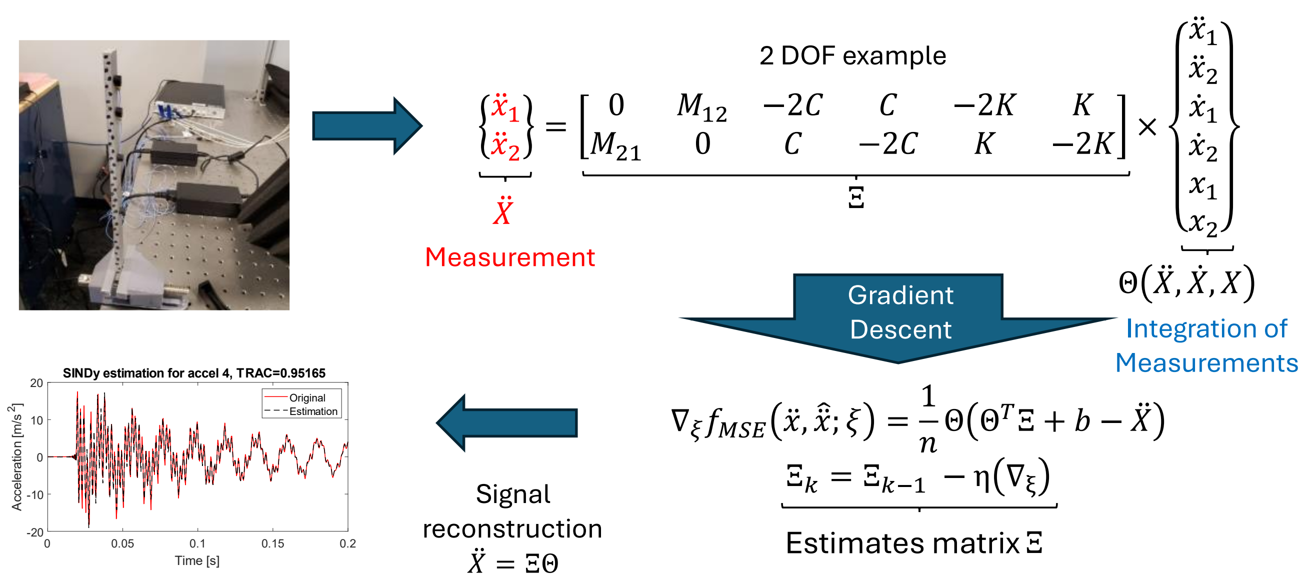

Fig. 1 Flowchart of proposed SINDy with stochastic gradient descent

$$\Xi_k = \Xi_{k-1} - \eta\left(\nabla_\xi\right) \tag{3}$$

where η is the learning rate and hyperparameter of the model. In addition, during the training, the values of the mass matrix which are equivalent to their respective results will be set to zero. Such that, it will prevent the optimization to obtain a trivial solution of $M_{ii}\ddot{X}_{ii} = M_{ii}\ddot{X}_{ii}$. In addition, considering that system identification is an ill-posed problem, with multiple possible solutions, extra information is required to obtain the correct system of equations. For instance, one of the physics terms added is related to the mass of the system. Multiple combinations of mass can be obtained for the same natural frequency and mode shape; therefore, the total mass of the system was required to obtain a more precise system of equations. From the total mass of the system ($\hat{M}$) it is assumed that the sum of the diagonal terms of the mass matrix should be the same value, as shown in Eq. (4).

$$\hat{M} = \sum_{i=1}^{n} M_{ii} \tag{4}$$

where, M_{ii} are the diagonal terms of the mass matrix and n is the number of DOF of the system. Later, the mass of the first DOF can be estimated based on the absolute error between the estimated mass and the total mass, as in Eq. (5).

$$M_{11}^{k+1} = M_{11}^{k} + \eta_m \left|\hat{M} - \sum_{i=1}^{n} M_{ii}\right| \tag{5}$$

Finally, assuming the parameters estimated on the optimization are normalized by the respective DOF mass, the other values of the mass matrix can be estimated based on Eq. (6).

$$M_{ii} = \frac{\xi_{i-1,i}}{\xi_{i.i-1}} \times M_{i-1,i-1} \tag{6}$$

where, ξ_{ij} is the term of the library at the i^{th} row and j^{th} column. Another penalty term added to the optimization problem is based on the eigenvalues of the system. Since the estimated PDE can have different natural frequencies than the original system (based on the eigen solution), the mean squared error of the estimated system is compared to the measurements. To obtain a penalty term in the SGD the gradient of the eigenvalue with respect to the stiffness matrix is given by Eq. (7) [14, 15].

$$\frac{d\lambda}{dK} = U^T \otimes U^T \tag{7}$$

where, λ is one of the eigenvalues of the system, K is the stiffness matrix, and U is its mode shape. Then the stiffness matrix can be updated based on the gradient of the error of the eigenvalue as presented in Eq. (8).

$$\nabla f_{MSE}\left(\lambda, \widehat{\lambda}\right) = \frac{1}{\lambda}\frac{d\lambda}{dK}\left(\lambda - \widehat{\lambda}\right) \tag{8}$$

Afterwards, a term was added to the optimization related to the symmetry of the matrices. It is known that for linear vibrational systems, the mass, damping, and stiffness matrices are symmetric. To encourage symmetry in the estimation, the penalty term (A_p) was implemented as described in Eq. (9).

$$A_p = \frac{\left[A - A^T\right]}{\|A\|} \tag{9}$$

where A can be either of the parameters from the library, such as mass, stiffness or damping. Finally, the loss function of the optimization problem is given by a combination of the four terms described previously, as presented in Eq. (10).

$$\mathcal{L} = \nabla_\xi f_{MSE}\left(\ddot{x}, \widehat{\ddot{x}}, \xi\right) + \alpha_1 \nabla f_{MSE}\left(\lambda, \widehat{\lambda}\right) + \alpha_2 f_{MAE}\left(M, \hat{M}\right) + \alpha_3 A_p \tag{10}$$

where, α_i are the weights for each of the parameters and must be fine-tuned depending on the application.

Simulation Results

The proposed algorithm will be employed into a cantilever beam which will be measured by four accelerometers. In order to validate the results obtained, a comparison with a Finite Element Model (FEM) will be performed. The FE model consists of a one hundred element cantilever beam, made of aluminum with the following properties:

Table 1 Cantilever beam properties

Property	Young's modulus (psi)	Width (in)	Thickness (in)	Length (in)	Mass density
Value	10^6	0.75	0.25	9.5	2.5×10^{-4}

The model was created considering the displacement and rotation of the elements, leading to the following mode shapes:

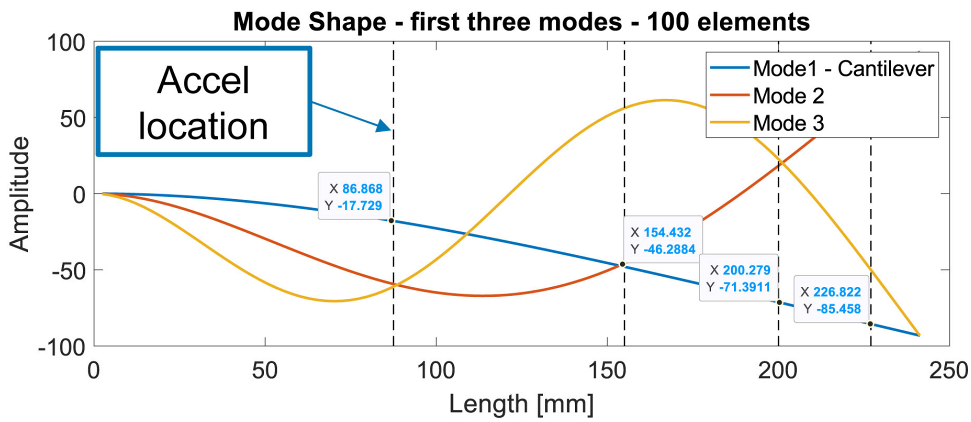

Fig. 2 Mode shapes obtained by FEM

After obtaining the mode shapes and natural frequencies from the simulation, the model was reduced into the same location of the accelerometers by using the System Equivalent Reduction Expansion Process (SEREP) [16]. The reduction of the model can be performed as shown in Eq. (11) below:

$$A_a^S = T_U^T A_n T_U \tag{11}$$

where A_a^S can be either the mass or stiffness matrix of the active set, A_n the matrix of the original model and T_U is the transformation matrix. Since the natural frequencies and mode shapes of the FE model differ from the measurements, a model update is required to represent the beam correctly. It was employed the stiffness and mass matrix analytical model improvement (KM-AMI) for the reduced model in order to obtain the correct governing equations for the system. The model improvement is calculated by Eqs. (12) and (13).

$$M_I = M_S + V^T \left[I - \overline{M}_S\right] V \tag{12}$$

where M_I is the improved mass matrix, M_S is the seed (or original) mass matrix, $\overline{M}_S$ is the orthogonal original mass matrix, however, instead of using the mode shapes obtained from the simulation, the measured mode shapes. Finally, V is a transformation matrix obtained from the measured mode shapes, the original mass matrix and $\overline{M}_S$.

$$K_I = K_S + V^T \left[\Omega^2 + \overline{K}_S\right] V - \left[K_S U_I V\right] - \left[K_S U_I V\right]^T \tag{13}$$

where similarly to the equation of the mass matrix, K_I, K_S and $\overline{K}_S$ are the improved and original stiffness matrices and the orthogonal stiffness matrix respectively. In addition, Ω^2 are the eigenvalues of the FEM and U_I its mode shapes. After performing the model reduction and updating it, its mode shapes are presented in Fig. 3. Since only three accelerometers were used for the SINDy estimation, the updated mode shapes only have three points, thus the plots do not look as smooth as the original FE simulation. It can be seen that the updated model and experimental results align very well, and in addition the natural frequencies of the mode shapes are the same for experimental and simulation.

The stiffness and mass matrices obtained after the model update will then be used as a metric to evaluate the parameters obtained by the SINDy algorithm. The values obtained from the FE model can be seen in Eq. (14) below:

$$M_{FEM} = \begin{bmatrix} 0.7 & -0.5 & 0.6 \\ -0.5 & 1.3 & -1.1 \\ 0.6 & -1.1 & 1.7 \end{bmatrix} \text{ and } K_{FEM} = \begin{bmatrix} 4.9 & -4.7 & 1.9 \\ -4.7 & 6.0 & -2.6 \\ 1.9 & -2.6 & 1.2 \end{bmatrix} 10^7 \tag{14}$$

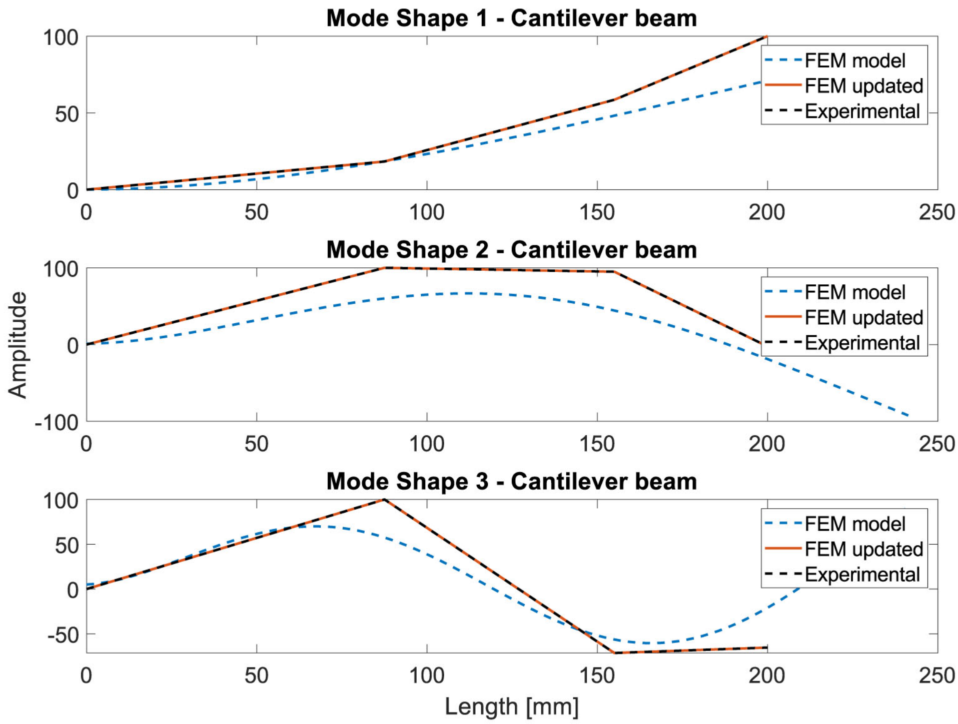

Fig. 3 Comparison of original simulation, updated model, and experimental mode shapes

Learning Results and Discussion

As a benchmark of the proposed methodology and the FEM simulation, the results presented next will be a comparison between the original approach for system identification and the physics-informed approach. Initially, the system identification using SINDy can be seen in Fig. 4.

As presented in the figure, the approximation of the first mode shape has a high accuracy, presenting 100% of modal assurance criteria (MAC) for the third and 99% for the fourth of the SINDy modes. However, when looking at the second mode shape, only the first of the estimated modes has good accuracy, with 75% MAC. When looking at the time reconstruction of the measurement it can be seen that for the accelerometers located in places where the first mode shape is predominant the accuracy of the time reconstruction is much higher, achieving above 90% of the time reconstruction assurance criteria

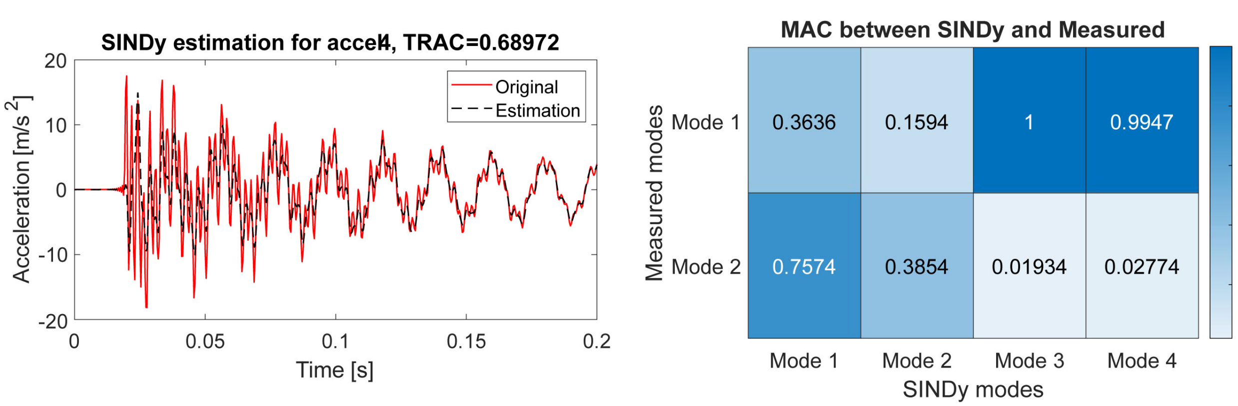

(a) (b)

Fig. 4 Result from original SINDy, (a) Signal reconstruction of accelerometer 4 and (b) MAC comparison with measurements

(TRAC). Meanwhile, for accelerometers such as accel 4, which is located in a region where higher frequency is predominant, the accuracy for TRAC is only 68%. Since the proposed approach uses an SGD approach, there are hyperparameters to be selected that will influence the final reconstruction, Table 2 shows the values selected for the hyperparameters.

Table 2 Hyperparameters for SGD SINDy training

Hyperparameter	**# of Epochs**	**Batch Size**	**Learning Rate**	**Mass LR**	α_{Freq}	$\alpha_{Symmetry}$
Value	10,000	128	1.5×10^{-4}	1.5×10^{-4}	0.1	1

After applying the same dataset into the proposed approach, the results are presented in Fig. 5.

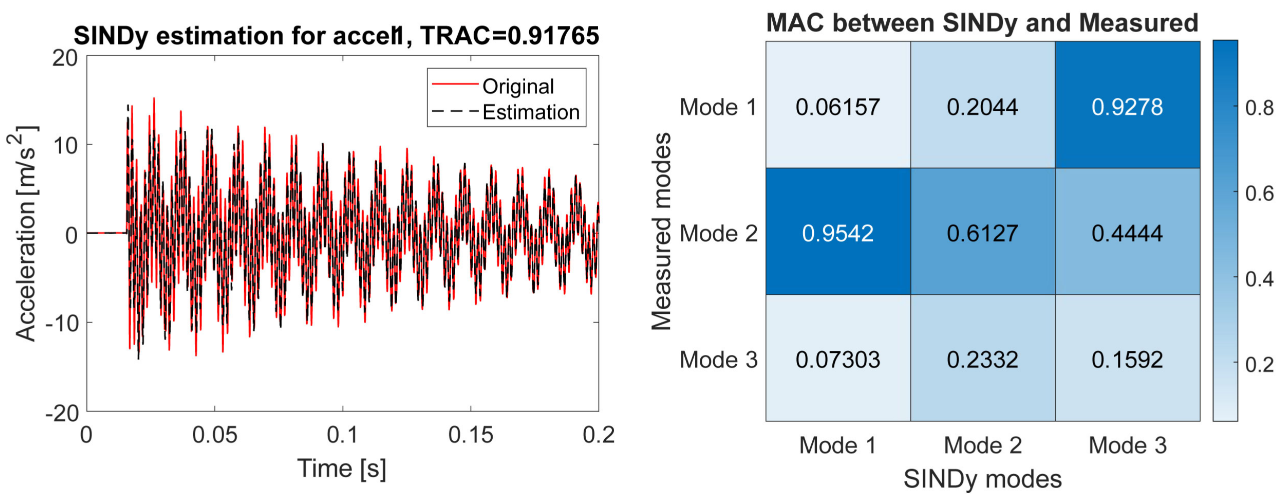

(a) (b)

Fig. 5 Results from SGD SINDy with penalty terms, (a) Signal reconstruction of accelerometer 1 and (b) MAC comparison with measurements

As presented in Fig. 5a, the proposed technique has a higher accuracy for accelerometers closer to the base of the beam, which will have higher frequency content available. For this case, a TRAC of 91% is obtained, furthermore, all other accelerometers have an accuracy above 90%. In addition, as presented in Fig. 5b, the mode shape reconstruction has higher than 90% MAC for both mode shapes 1 and 2. Unfortunately, due to the numerical damping caused by the integration of the acceleration, the third mode shape could not be obtained. In addition to the signal reconstruction and MAC, the matrices are compared between a finite element (FE) model and the SINDy estimation. The mass and stiffness matrices for SINDy are presented in Eq. (15) below.

$$M_{SINDy} = \begin{bmatrix} 0.0409 & -0.0395 & 0.0086 \\ -0.0395 & 0.0425 & -0.0058 \\ 0.0080 & -0.0058 & 0.0165 \end{bmatrix} \text{ and } K_{SINDy} = \begin{bmatrix} -1.825 & 0.764 & -2.039 \\ 0.753 & -1.683 & 5.678 \\ -2.064 & 5.658 & 1.733 \end{bmatrix} 10^3 \quad (15)$$

As shown in Eq. (15), the off-diagonal terms in the matrices are similar, differing only two digits after the decimal for the stiffness matrix. Leading to a behavior that is expected for a linear vibrational system. In addition, the difference between the values obtained by SINDy and the FE model is computed, following Eq. (16), where the absolute error is calculated based on the normalized values of each matrix.

$$Error_A = \frac{[A]_{FEM}}{\|[A]_{FEM}\|} - \frac{[A]_{SINDy}}{\|[A]_{SINDy}\|} \quad (16)$$

Figure 6 presents the computed error between the FE model and the SINDy estimation for the mass matrix (a) and the stiffness matrix (b). It can be noticed that although the SINDy model obtains a symmetric result for the system for both matrices, the proportions of the matrix are different when compared to the FE model. For instance, the highest value of the FE model stiffness matrix is on the last DOF, while for the SINDy estimation, it happens in the first DOF.

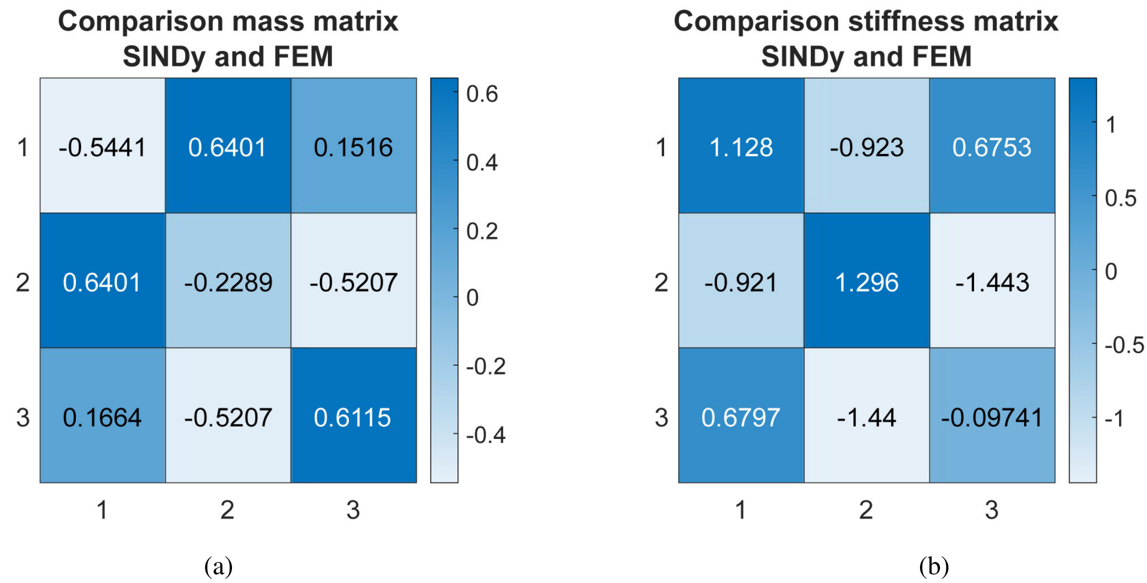

Fig. 6 Comparison of (a) mass and (b) stiffness matrices between FE model and SINDy estimation

Conclusion

This study presents a variation of the SINDy algorithm developed by Brunton et al. [5], for application on second order PDEs, specifically vibrational systems. Results for original SINDy show acceptable approximation for governing equation estimation, however, due to the dependence between variables in the problem, it becomes challenging to correctly predict mode shapes and natural frequencies of the structures. The modifications in the algorithm allow a better estimation of both natural frequencies and mode shapes, while increasing the signal reconstruction obtained by the estimated parameters. While the PDEs estimated using SINDy are not the same as the ones obtained by a simplified FE model, the proposed approach suggests a good approximation of the system, with a small number of assumptions that can be easily obtained by measurements.

For future work, more improvements for the algorithm can be performed, for instance the current version works best for free vibration measurements (obtained by impact test). When different excitation is given, e.g. random excitation, the governing equations identification poses to be challenging. In addition, more tests can be performed in more complex structures, including nonlinear structures to observe how the approach will behave when dealing with more parameters to be estimated.

Acknowledgments This work is supported by the Department of Energy Kansas City National Security Campus Managed by Honeywell under contract # N000510678. NSC-614-5662 10/2024. Unclassified Unlimited Release

References

1. O. Nelles and O. Nelles, *Nonlinear dynamic system identification*. Springer, 2020.
2. F. Abdullah and P. D. Christofides, “Data-based modeling and control of nonlinear process systems using sparse identification: An overview of recent results,” *Computers & Chemical Engineering*, vol. 174, p. 108247, 2023.
3. T. Liu and H. Meidani, “Physics-informed neural networks for system identification of structural systems with a multiphysics damping model,” *Journal of Engineering Mechanics*, vol. 149, no. 10, p. 04023079, 2023.
4. M. Raissi, P. Perdikaris, and G. E. Karniadakis, “Physics-informed neural networks: A deep learning framework for solving forward and inverse problems involving nonlinear partial differential equations,” *Journal of Computational physics*, vol. 378, pp. 686-707, 2019.
5. S. L. Brunton, J. L. Proctor, and J. N. Kutz, “Discovering governing equations from data by sparse identification of nonlinear dynamical systems,” *Proceedings of the national academy of sciences*, vol. 113, no. 15, pp. 3932-3937, 2016.
6. C. Lathourakis and A. Cicirello, “Physics-enhanced sparse identification of nonlinear oscillator with coulomb friction,” in *International Conference on Nonlinear Dynamics and Applications*, 2023: Springer, pp. 507-517.
7. C. Lathourakis and A. Cicirello, “Physics enhanced sparse identification of dynamical systems with discontinuous nonlinearities,” *Nonlinear Dynamics*, pp. 1-28, 2024.

8. S. Piramoon, M. Ayoubi, and S. Bashash, “Modeling and Vibration Suppression of Rotating Machines Using the Sparse Identification of Nonlinear Dynamics and Terminal Sliding Mode Control,” *IEEE Access*, 2024.
9. S.-C. Huang, H.-W. Chen, and M.-H. Tien, “Predicting Nonlinear Modal Properties by Measuring Free Vibration Responses,” *Journal of Computational and Nonlinear Dynamics*, vol. 18, no. 4, p. 041005, 2023.
10. K. Kaheman, J. N. Kutz, and S. L. Brunton, “SINDy-PI: a robust algorithm for parallel implicit sparse identification of nonlinear dynamics,” *Proceedings of the Royal Society A*, vol. 476, no. 2242, p. 20200279, 2020.
11. P. Goyal and P. Benner, “Discovery of nonlinear dynamical systems using a Runge–Kutta inspired dictionary-based sparse regression approach,” *Proceedings of the Royal Society A*, vol. 478, no. 2262, p. 20210883, 2022.
12. Y. Liu, S. Shi, Y. Fang, and A. Fu, “Robust data-driven wave excitation force estimation for wave energy converters with nonlinear probabilistic modelling,” *Ocean Engineering*, vol. 310, p. 118726, 2024.
13. S. H. Rudy, S. L. Brunton, J. L. Proctor, and J. N. Kutz, “Data-driven discovery of partial differential equations,” *Science advances*, vol. 3, no. 4, p. e1602614, 2017.
14. J. R. Magnus, “On differentiating eigenvalues and eigenvectors,” *Econometric theory*, vol. 1, no. 2, pp. 179-191, 1985.
15. A. D. Belegundu and T. R. Chandrupatla, *Optimization concepts and applications in engineering*. Cambridge University Press, 2019.
16. R. Allemang and P. Avitabile, *Handbook of experimental structural dynamics*. Springer Nature, 2022.